

# Effect of the Mini Perforated Resistance on Heat Transfer and Pressure Loss

Irfan Kurtbas

Department of Mechanical Engineering  
Hitit University  
Corum, Turkey  
[ikurtbas@gmail.com](mailto:ikurtbas@gmail.com)

Alptug Yataganbaba

Department of Mechanical Engineering  
Hitit University  
Corum, Turkey  
[alptugyataganbaba@gmail.com](mailto:alptugyataganbaba@gmail.com)

Mehmet Sener

Department of Mechanical Engineering  
Hitit University  
Corum, Turkey  
[mehmetsener@hitit.edu.tr](mailto:mehmetsener@hitit.edu.tr)

**Abstract**—As is known the heat transfer enhancement techniques are broadly classified into two groups: active and passive techniques. In this study, it is aimed to increase heat transfer by using passive method in a channel exposed to constant heat flux. For this purpose, a flow channel which 8x40x50mm in size was heated with constant heat flux from bottom surface. The copper resistances which have the mini flutes in different steps were placed on heating surface. Resistances were bonded with very low thermal resistance artice silver adhesive to form fin effect on heater surface. Four different resistance steps and channel width ratios ( $t=0.071$ ,  $t=0.12$ ,  $t=0.2$  and  $t=0.33$ ) were preferred. There are 72 and 78 holes which 0,02x0,6 mm in size in each resistance step (on each surface). Experiments were performed at 7 different flow rates and within Reynolds number range from 3350 to 22600. Temperature and hence local heat transfer coefficient were obtained via measuring the temperature distribution on the heating surface by thermal camera. Depending on the configuration of resistances, heat transfer and pressure loss were determined. In experimental findings, heat transfer and pressure loss decreased with increasing aspect ratio of resistance.

**Keywords**—heat transfer, pressure loss, mini resistance

## I. INTRODUCTION

Turbulent flows are characterized by using of turbulence generators determining the hydrodynamic behavior of the system. As is known, boundary layer inside fully developed flow and the velocity distribution in the bottom boundary layer significantly change the transfer coefficient of fluid. This type of flow is encountered in many systems, such as heat exchangers, gas-cooled reactor fuel elements, electronic systems and car radiators [1]. A considerable amount of literature has been published on the theoretical and experimental investigation of the flow in the rotational flow. The study of the useful effects of turbulence generators on the heat transfer was first carried out by Royds [2]. In another major study, Demirtas et al. [3] examined the effects of conical ring surface elements which were placed in cylindrical tubes on the heat transfer by a number of experimental studies. They found 80% increase in heat transfer and an increase in pressure loss. Ekkad et al. [4] investigated the convective heat transfer

coefficient in two-pass smooth rectangular channel which has rib turbulators in detail. Flaps were placed on the channel surface. 60° and 90° angle flaps are mounted different configurations such as parallel, V ribs and V inverted ribs. Thus, the heat transfer increased by 20-25 % compared with empty tube. The effects of angled, transverse, discrete, angled discrete, V-shaped, V-shaped broken and parallel broken ribs were investigated on heat transfer as previously reported by Tanda [5]. A liquid crystal thermography technique (LCT) was used for local transport coefficient. The reverse flow was generated by changing flow direction placed with 45-60° transverse and V-shaped ribs to flow direction. As a result, heat transfer and pressure loss substantially changed depending on rib shape and geometry. Boomsma et al. [6] performed experiments into a compact heat exchanger with manufactured from 6001-T6 alloy open-cell aluminum foam. The study revealed that the metal foam heat exchangers decreased the thermal resistance by nearly half in comparison to conventional heat exchangers designed for the same applications.

Researchers, who have considerably modified the materials of conventional heat exchangers, compared their results with the outcomes of compact heat exchangers used for commercial purposes. In another work, a concentric heat exchanger with snail entrance was placed to generate fading flow model in the inlet pipe by Durmus et al. [7]. It is therefore desirable to further enhance the heat transfer performance. Experimental results showed that swirling angles were the most important parameters on the heat transfer and pressure loss. Durmus et al. [8] reported the influence of co-axis free rotating propeller-type turbulators on the performance of a heat exchanger. The effect of the blade angle, blade diameter, the number of fins and the distance between turbulators of the propeller fin turbulators on heat transfer was investigated. Yildiz et al. [9] studied the effect of rotary heat exchanger on the heat transfer and pressure loss. This first type of heat exchanger consisted of two tubes nested concentrically. Other heat exchanger consisted of pipes containing different pitches opening into the outer surface of the inner tube. During the experiments, while hot fluid was transferred from outer surface of inner tube, cold fluid was transferred from inner surface of inner tube. They reported 100% increase in the Nusselt number. At the same time, it was stated that the rate of heat transfer could be increased further by increasing pitch number of the twists.

In this study, the effect of mini perforated resistances on the heat transfer and pressure loss in the flow channel were investigated experimentally. Copper was used as resistance material. The effect of resistance step on heat transfer and pressure loss in addition to different number and arrangement of ribs was also determined.

## II. EXPERIMENTAL SETUP AND METHODS

The schematic representation of the test facility used for this experimental study is shown in Fig. 1. Test section had a length of 51mm and width of 219 mm. The height was changed according to resistance height. The resistance wall thickness was 0.12 mm. Resistances were fixed on the 0.02 mm thickness stainless steel film heater with the help of Artic-silver adhesive. Heat flux control of the film heater was provided by an AC power supply. AC power supply can produce maximum 6V and 110A and it can be changed optionally. Test section was made from the plexiglass. The length about 10 times of the test channel and the same hydraulic diameter with test section was left to ensure the full development of the flow at the input of the channel. A fan (2.2 kW and 3000 rpm) was used to provide air to be heated. Different mass flow rates were provided with changing the fan speed by Vacon's type frequency convector. Air to be heated was provided by suction to prevent turbulence affect caused by the discharge of air. The air velocity was measured by the Kimo LV107 type anemometer (70 mm diameter) connected to the output of fan. In the experimental set, temperatures on the heater surface, the input and output of the test section were measured by Flir A645 type thermal camera and calibrated type k thermocouples, respectively. The inlet and outlet air temperatures in the test section were measured from four different points and determined by finding the average of them. Thermocouples were connected to OMEGA HH21 type digital micro-voltmeter. AIMEMO 2950 and pressure transducer were used to determine the pressure drop between the air inlet and outlet at the test section. The temperatures at the inlet, outlet and the surface of the heater, the flow rate, and pressure difference of fluid flowing through the test section were measured and recorded throughout the experimentation. Designed resistance illustrated in Fig. 2. Resistances were made of copper sheet with a thickness of 0.12mm. Measurements of resistances are shown in Table I.

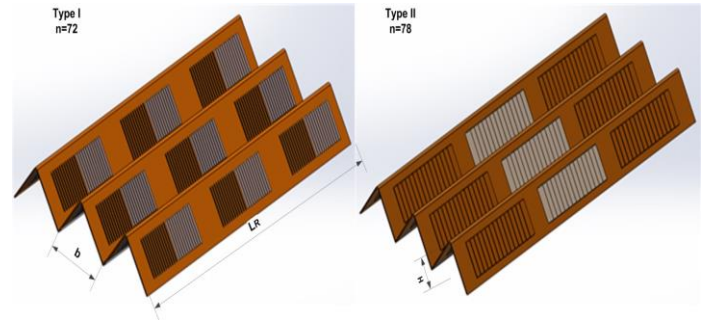


Fig. 2. Detailed view of the resistances

Table I. Measurement of resistances (mm)

	Type I	Type II
$t=(b/W)$	0.071, 0.12, 0.2, 0.33	0.071, 0.12, 0.2, 0.33
H (mm)	5.41, 6.77, 7.23, 7.58	3.85, 5.23, 6.61, 6.8
$L_c$ (mm)	104	120
n (times)	72 (for each surface)	78 (for each surface)

### Uncertainty Analysis

All experiments and measurements were repeated several times in order to reduce the measurement errors and to increase the reliability of the results. A detailed error analysis is made to estimate the  $w_R$  uncertainty arising from different independent variables from the following equation, as adapted from Reference [10];

$$w_R = \left[ \left( \frac{\partial R}{\partial x_1} w_1 \right)^2 + \left( \frac{\partial R}{\partial x_2} w_2 \right)^2 + \dots + \left( \frac{\partial R}{\partial x_n} w_n \right)^2 \right]^{1/2} \quad (1)$$

where R,  $x_1, x_2, \dots, x_n$  is a function of the independent variables.  $w_1, w_2, w_n$  is the uncertainty of the independent variable [11]. The uncertainties associated with the experimentally measured and calculated properties are demonstrated in Table II.

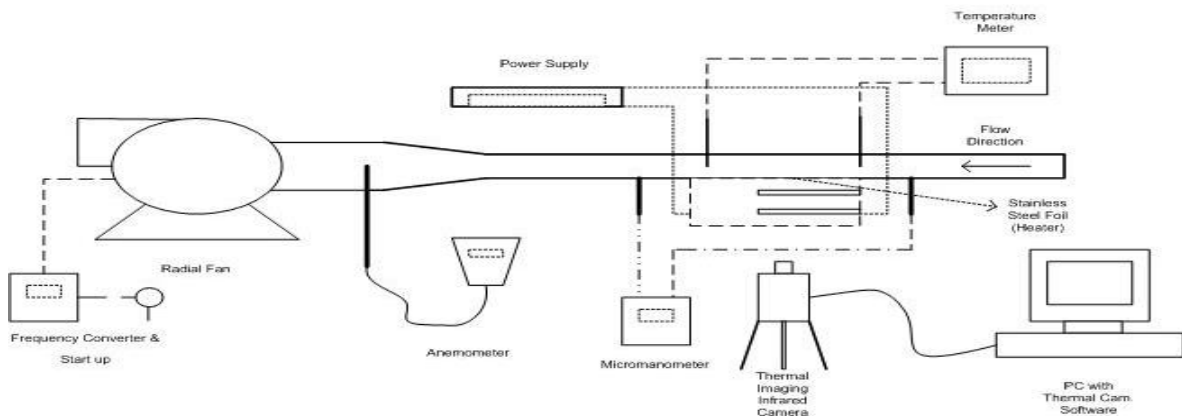


Fig 1. Schematic diagram of experimental setup

Table II. Uncertainties of total variables

Parameter	Total (%)
Nusselt number	±3.4
Reynolds number	±2.8
Coefficient of friction	±4.1
Effectiveness	±4.1
NTU	±4.8

Total uncertainty value for the coefficient of friction with using equation (1):

$$w_f = \left[ \left( \frac{\partial f}{\partial \Delta P} w_{\Delta P} \right)^2 + \left( \frac{\partial f}{\partial D_H} w_{D_H} \right)^2 + \left( \frac{\partial f}{\partial V} w_V \right)^2 + \left( \frac{\partial f}{\partial L} w_L \right)^2 \right]^{1/2} \quad (2)$$

The total uncertainty for the friction coefficient can be written with rearranging equation (2);

$$\frac{w_f}{f} = \left[ \left( \frac{w_{\Delta P}}{\Delta P} \right)^2 + \left( \frac{w_{D_H}}{D_H} \right)^2 + 4 \left( \frac{w_V}{V} \right)^2 + \left( \frac{w_L}{L} \right)^2 \right]^{1/2} \quad (3)$$

Other uncertainties are obtained in the same way.

### III. RESULTS

Fig. 3 shows the experimental data for the Nusselt number with different Reynolds numbers at the turbulators with 60° blade angle. Values such as density, specific heat and viscosity are defined according to the arithmetic average of the inlet-outlet temperature of air when variables calculating. In each turbulator experiment, small changes in the Reynolds number of the same mass flow rate occurred because of various temperature differences. This change is not taken into account in the chart.

Reynolds number is defined as the ratio of inertial forces to viscous forces, and is defined as follows;

$$Re = \frac{\rho \cdot V \cdot D_H}{\mu} \quad (4)$$

Nusselt number is equal to dimensionless temperature gradient on the surface and gives a measure of the convective heat transfer formed on the surface, and is given by;

$$Nu_m = \frac{h_m \cdot D_H}{k} \quad (5)$$

where  $D_H$  equivalent (hydraulic) diameter can be expressed as follows;

$$D_H = \frac{4 \cdot A_k}{P} = \frac{2 \cdot H \cdot W}{(H + W)} \quad (6)$$

The average transfer coefficient of air;

$$h_m = \frac{Q_g}{A_y \cdot LMTD} = \frac{\dot{m} \cdot C_p \cdot (T_c - T_g)}{A_y \cdot LMTD} \quad (7)$$

is calculated with the correlation.

For the friction coefficient;

$$f = \frac{2 \cdot g \cdot \Delta P}{V^2} \cdot \frac{D_H}{L_b} \quad (8)$$

correlation is used.

In a heat exchanger, the effectiveness of a heat exchanger is generally given by NTU (Number of Transfer Unit) method. The effectiveness of a heat exchanger is defined as the ratio of actual heat transfer rate to the maximum possible heat transfer rate and, is given by;

$$\varepsilon = \frac{Q_g}{Q_{\max}} \quad (9)$$

The number of switching units, indicated by NTU (Number of Transfer Unit) are widely used in heat exchanger analysis, wherein,

$$NTU = \frac{A_y \cdot U}{C} \quad (10)$$

defined this format is a dimensionless parameter. Where C is the thermal capacity of the fluid and it is equal to the product of mass flow rate and specific heat [12].

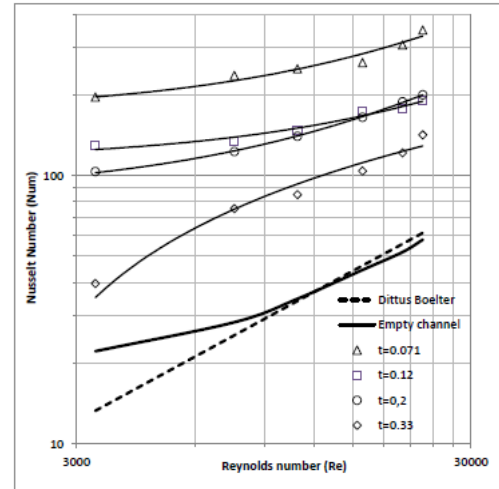


Fig. 3. Variation of the Nusselt number as a function of Reynolds number for type I

Empty channel experiments are performed and compare with theoretical values to ensure the validity of experimental findings. Dittus-Boelter equation for Nusselt number and Blasius correlation for the coefficient of friction are used from the equations given in the literature, and are calculated as follows;

$$Num = 0.023 \cdot Re^{0.8} \cdot Pr^{0.4} \quad (11)$$

and

$$f = 0.316 \cdot Re^{-0.25} \quad (Re \leq 2 \cdot 10^4) \quad (12)$$

The results which obtained from empty channel experiments have very close values with the theoretical Dittus-Boelter equation. As shown in Fig. 3, the heat transfer at type I resistance for  $t=0.071$  increases nearly 8 times at minimum

Reynolds number, 6 times at maximum Reynolds number compared with empty channel. Accordingly, the mean Nusselt number ranges from 196 to 350. These values range from 129 to 190 when  $t = 0.12$ . The rate of increase varies between 3.3-5.8 times.

In Fig.4, the variation of friction coefficient with different Reynolds number is given for type I resistances. Heat transfer and pressure losses are found to be proportional throughout the experiments. Namely, the heat transfer and pressure loss increases together depending on the resistance. It can be seen, friction coefficient increases about 6.3-17.5 times according to empty channel when  $t=0.071$ , about 3.6-7.9 times when  $t=0.12$ , about 2.9-6.4 times when  $t=0.2$  and about 2-5.8 times when  $t=0.33$ .

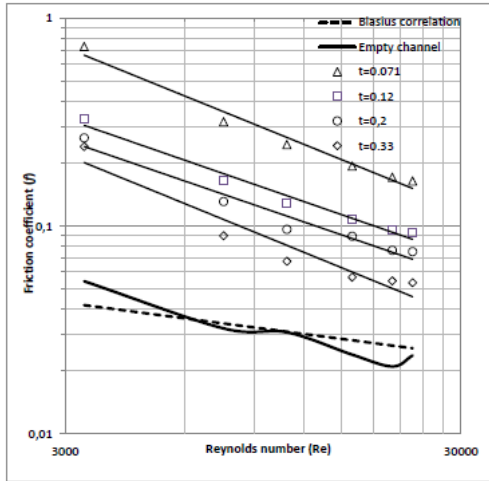


Fig. 4. Variation of the friction coefficient as a function of Reynolds number for type I

As shown in Fig. 5, the heat transfer at type I resistance increases about 5-11 times when  $t=0.071$  depending on Reynolds number compared with empty channel. Average Nusselt number also decreases with decreasing  $t$  value. According to empty channel, Nusselt number reduces by up to approximately 1.2 times. Thus, average Nusselt number is obtained as 340 at minimum and 340 at maximum.

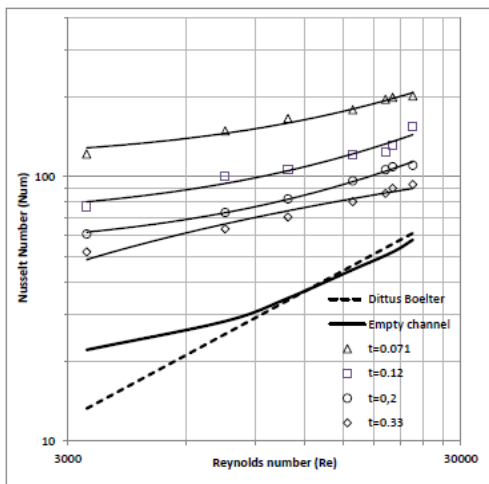


Fig. 5. Variation of the Nusselt number as a function of Reynolds number for type II

The variation of friction coefficient with different Reynolds number for type II resistance is given in Fig. 6. Heat transfer and pressure loss show a similar change compared with type I experiments. It can be seen, friction coefficient increases about 20 times according to empty channel when  $t=0.071$ , about 9 times when  $t=0.12$ , about 8.5 times when  $t=0.2$  and about 6 times when  $t=0.33$ .

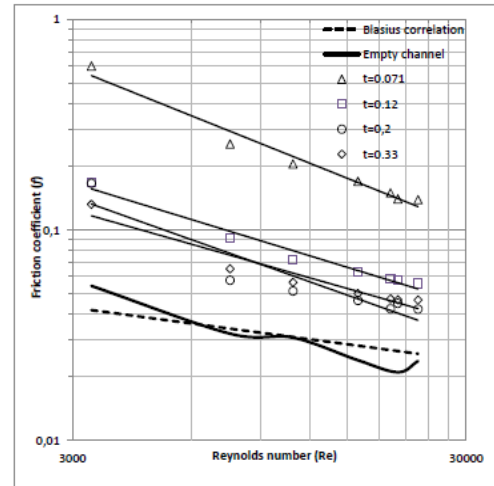


Fig. 6. Variation of the friction coefficient as a function of Reynolds number for type II

As a result of total experiments, empirical formulas are obtained for Nusselt number and friction coefficient containing independent parameters by using values obtained for each variable. In these empirical correlations, coefficients of variables are obtained by using the method of multiple regressions as follows;

Nusselt number ( $Nu_m$ ) for type I;

$$1.55.Re^{0.28}.(t)^{-0.997} Pr^{0.4} (R^2=0.98) \quad (13)$$

Friction coefficient (f)

$$18.23 Re^{-0.853} (t)^{-1.44} Pr^{0.4} \quad (14)$$

Nusselt number for type II ( $Nu_m$ )

$$1.91.Re^{0.26}.(t)^{-1.03} Pr^{0.4} (R^2=0.98) \quad (15)$$

Friction coefficient (f)

$$19.88 Re^{-0.88} (t)^{-1.39} Pr^{0.4} \quad (16)$$

These equations obtained from the method of multiple regressions are in line with the experimental results with the error rate of Nusselt number for  $\pm 10\%$  and  $\pm 8\%$  for the friction coefficient.

As shown in Fig. 7, NTU ranges from 2.5 to 0.4 according to the results of empty channel experiments. The power is 2400W in the designed system. Effectiveness of empty channel changes  $0.09 < NTU < 0.22$  range according to equation

(9). On the other hand, it can be seen that designed turbulators increase the effectiveness of the heat exchanger about 1.9-2.28 times. Therefore, number of transfer unit (NTU) changes from 0.6 to 1.35.

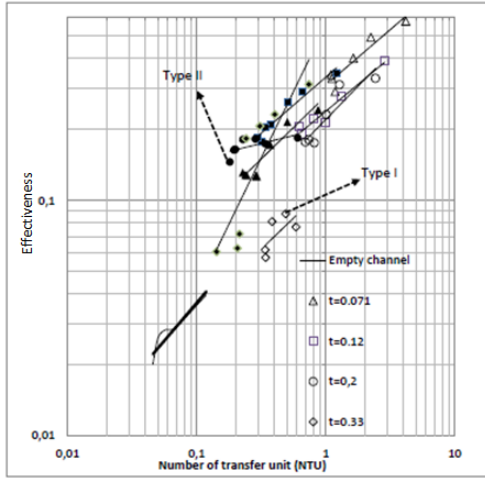


Fig. 7. Variation of the effectiveness as a function of NTU for type I and type II

In this study, the change of the effectiveness according to NTU is preferred to represent with empirical equations instead of showing with graphics.

Effectiveness for type I ( $\epsilon$ )

$$=(0.281.(NTU)^{0.27} \cdot (t)^{-0.278}) - 0.276 \quad (R^2=0.978) \quad (17)$$

Effectiveness for type II ( $\epsilon$ )

$$=(1.102.(NTU)^{0.089} \cdot (t)^{-0.071}) - 1.006 \quad (R^2=0.971) \quad (18)$$

Equation (17) and (18), is valid for  $0.1 < NTU < 4.2$  range. As shown in Fig. 7, NTU is the most important parameter on efficiency. Equation (17) is obtained by multiple regressions however; up to 18% error has occurred at the maximum and minimum values of NTU. Therefore, a constant number subtracts from effectiveness value.

#### IV. CONCLUSION

The aim of this experimental study is to prevent the formation of boundary layers at regular intervals (continuous help of mini- holes) and extend the flow path of the fluid to be heated using passive methods with the help of designed resistance. Thus, the purpose is to increase the temperature difference of the fluid to be heated. According to the values obtained from the experiments, designed resistances increased the air outlet temperature compared with empty channel by up to 8 times. Besides, resistance used in the experiments increased by up to 20 times at maximum compared with empty channel due to creating resistance in the flow media. As is known, the pressure loss increases energy loss due to pump power.

In this study, the effect of designed resistance on heat transfer and frictional losses are defined and empirical formulas are provided for the literature. As shown in graphics and empirical formulas, heat transfer is proportional to the Reynolds number and the number of holes, whereas it is inversely proportional to resistance step. Moreover, friction loss is inversely proportional to both Reynolds number and resistance step.

#### SYMBOLS

$A_k$	the channel cross-sectional area ( $m^2$ )
$A_y$	the channel heating surface area ( $m^2$ )
$b$	resistance step (m)
$C_p$	specific heat (kJ/kg.K)
$C$	heat capacity (W/K)
$D_H$	hydraulic diameter (m)
$f$	friction coefficient (-)
$g$	acceleration of gravity ( $m/s^2$ )
$h_m$	average convection coefficient ( $W/m^2.K$ )
$k$	conduction coefficient ( $W/m.K$ )
$L_C$	channel length (m)
$L_R$	resistance length (m)
$Nu$	nusselt number (-)
$NTU$	number of transfer unit (-)
$Q_g$	heat gain (W)
$Q_{max}$	maximum possible heat transfer rate (W)
$U$	overall heat transfer coefficient ( $W/m^2.K$ )
$Re$	reynolds number (-)
$V$	The average speed of the air (m/s)
$\Delta P$	pressure difference (m)
$m$	mass flow rate (kg/s)
$\rho$	density ( $kg/m^3$ )
$\epsilon$	effectiveness (-)

#### REFERENCES

- [1] J. Marie Buchlin, Convective heat transfer in a channel with perforated ribs, *Int. J. Therm. Sci.*, vol. 41, pp. 332-340, 2002.
- [2] R. Royds, Heat Transmission by Radiation, Conduction and Convection (1<sup>st</sup> Ed), pp 191-201 Constable and Comany, London, 1921.
- [3] C. Demirtaş, A. Durmuş, T. Ayhan and H. Karabay, The effects of conical ring surface of the diffuser on boiler efficiency, 25-28 May, Akdeniz University 1992.
- [4] S.V. Ekkad, Y. Huang and J.C. Han, Detailed heat transfer distributions in two-pass square channels with rib turbulators and bleed holes, *Int. J. Heat Mass Transfer*, vol 41, pp. 3781-3791, 1998.
- [5] C. Tanda, Heat transfer in rectangular channels with transverse and V-shaped broken ribs, *Int. J. Heat Mass Transfer*, vol. 47, pp. 229-243, 2004.
- [6] K. Boomsma, D. Poulikakos and F. Zwick, Metal foams as compact high performance heat exchangers, *Mechanics of Materials*, vol. 35, pp. 1161-1176, 2003.
- [7] A. Durmuş, A. Durmuş and M. Esen, Investigation of heat transfer and pressure drop in a concentric heat exchanger with snail entrance, *Applied Thermal Engineering*, vol. 22, pp. 321-332, 2002.
- [8] A. Durmuş, İ. Kurtbaş, F. Gülçimen and E. Turgut, Investigation of the effect of co-axis free rotating propeller type turbulators performance of heat exchanger. *Int. Communications in Heat and Mass Transfer*, vol. 31, pp. 133-142, 2004.
- [9] C. Yildiz, Y. Bicer, D. Pehlivan, Heat transfer and pressure drop in a heat exchanger with a helical pipe containing inside wires. *Energy Conversion and Management*, vol. 38, pp. 619-624, 1997.
- [10] J.P. Holman, *Experimental Methods for Engineers* (6<sup>st</sup> Ed.), McGraw-Hill, pp. 48-143, Signapore, 1994.
- [11] A. Hepbaşlı, O. Akdemir, Energy and exergy analysis of a ground source (geothermal) heat pump system, *Energy conversion and Management*, 45, pp. 737-753, 2004.
- [12] F.P. Incropera and D.P. DeWitt, *Fundamentals of Heat and Mass Transfer*, 2001.

